Neutron Scattering from Liquid Argon

B. A. DASANNACHARYA* AND K. R. RAO*
Physics Division, Atomic Energy of Canada Limited, Chalk River, Ontario, Canada
(Received 4 August 1964)

Extensive measurements of slow-neutron inelastic scattering from liquid argon at 84.5°K have been made using cold and thermal neutrons. The cold-neutron experiments were performed using a rotating-crystal spectrometer. A triple-axis spectrometer in its "constant-Q" mode of operation was used for the thermal-neutron measurements. A wave-vector transfer (Q) range of 0.4 to 6.0 Å^{-1} was covered, a range which extends through the third peak in the diffraction pattern of liquid argon. Some data were also collected at 87.9°, 90.0° and 92.3°K. The measurements at 84.5°K were converted to Van Hove's $S(Q, \omega)$ which was in turn converted to the intermediate scattering function, $I(Q, t)$, and then to Van Hove's space-time self- and pair-correlation functions. $I(Q, t)$ was determined for $Q \leq 6$ Å^{-1} and $t \leq 6\times10^{-12}$ sec. The self-correlation function, $G_s(r, t)$, has been completely mapped in the time range $0-2\times10^{-12}$ sec and is found to be Gaussian in shape to within our experimental accuracy (about 10 to 15%). The width of $G_s(r, t)$ follows the law obtained by assuming Fick's law for diffusion to hold. This suggests that in argon diffusion is a simple process, unlike that in other liquids investigated by means of neutrons. This conclusion is also supported by measurements on the temperature dependence of the energy width. These measurements give an activation energy of roughly 700 cal/mole for diffusion, in fair agreement with previous measurements on the temperature dependence of the diffusion constant. The time-dependent pair-correlation function has also been determined in the time range of $0-2\times10^{-12}$ sec. From 2×10^{-12} to 6×10^{-12} sec, a weighted combination of $G_s(r, t)$ and $G_d(r, t)$ is observed. The static pair-correlation function is in agreement with earlier measurements on argon and krypton.

INTRODUCTION

In recent years considerable interest has arisen in studies of scattering of slow neutrons from liquids with a view to understand the dynamical behavior of substances in the liquid state. In the now well-known paper, Van Hove[1] pointed out that by detailed measurements of energy and momentum transfers of monochromatic neutrons scattered from a liquid one can arrive at the time-dependent correlation functions for the liquid. He further showed that the self- and pair-correlation functions, defined by him, have simple physical meanings for classical liquids. The first measurements reported were those of Brockhouse[2] on water —an easily available incoherent scatterer. Later investigations were carried out on several hydrogenous liquids largely because of interest in them as moderators in nuclear reactors. Measurements have been reported on several liquid metals—lead,[3,4] tin,[4,5] and sodium.[6] These substances were found to have a comparatively complicated dynamical behavior in the liquid state. We undertook the measurement of neutron-scattering from liquid argon for the reason that argon is probably the simplest liquid to understand theoretically. The interatomic potential for argon is known from the studies in the gaseous and solid state. A first attempt has already been made by DeGennes[7] to describe the behavior of scattering of slow neutrons from liquid argon, under the assumption of a Gaussian velocity correlation function.

We have carried out extensive measurements of energy distributions of neutrons scattered from a thin sample of liquid argon at 84.5°K under its saturated vapor pressure of 550 mm of mercury. A range of wave-vector transfer $\mathbf{Q}$ from 0.4 to 6.0 Å^{-1} was covered in these measurements by using the rotating crystal and the triple axis spectrometers at the NRU reactor. A few measurements were also made at higher temperatures on the rotating crystal spectrometer. In Sec. II of this paper we briefly review the relevant parts of Van Hove's theory of neutron scattering from liquids. In Sec. III the apparatus and details of the experiment are described and the experimental observations are presented. Section IV describes the procedure followed for analyzing the experimental data and presents the main results—the intermediate scattering function and the time-dependent correlation function. In the final section, the conclusions—the effect of coherent scattering, the behavior of the intermediate scattering function and the correlation functions—are summarized. The shape of the self-correlation function is found to be Gaussian within experimental errors and the study of its width suggests that the diffusion is a simple process in liquid argon, following Fick's law of diffusion even for times as small as $\sim5\times10^{-13}$ sec.

II. THEORY

The partial differential cross section of neutrons of initial energy E_0, scattered with an energy change $\hbar\omega$

* Visiting scientist from Atomic Energy Establishment Trombay, Bombay, India, now returned.

[1] L. Van Hove, Phys. Rev. **95**, 249 (1954).

[2] B. N. Brockhouse, Nuovo Cimento Suppl. **9**, 45 (1958).

[3] B. N. Brockhouse and N. K. Pope, Phys. Rev. Letters **3**, 259 (1959).

[4] H. Palevsky in *Inelastic Scattering of Neutrons in Solids and Liquids* (International Atomic Energy Agency, Vienna, 1961), p. 265.

[5] S. J. Cocking and Z. Guner, in *Inelastic Scattering of Neutrons in Solids and Liquids* (International Atomic Energy Agency, Vienna, 1963), Vol. 1, p. 237.

[6] S. J. Cocking, in *Inelastic Scattering of Neutrons in Solids and Liquids* (International Atomic Energy Agency, Vienna, 1963), p. 227.

[7] P. G. DeGennes, Physica **25**, 825 (1959).

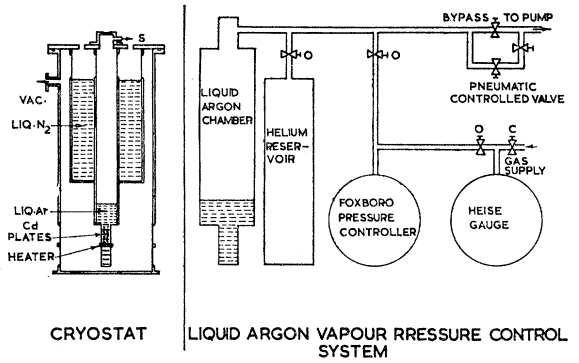

FIG. 1. Flow diagram of the liquid argon setup.

into an energy interval $\hbar d\omega$ and a solid angle $d\Omega$ is given by[1]

$$\frac{d^2\sigma_{\rm inc}}{d\omega d\Omega}=\frac{N[\langle b^2\rangle-\langle b\rangle^2]}{2\pi}\cdot\frac{k'}{k_0}\cdot S_{\rm inc}(\mathbf{Q},\omega) \tag{1a}$$

and

$$\frac{d^2\sigma_{\rm coh}}{d\omega d\Omega}=\frac{N\langle b\rangle^2}{2\pi}\cdot\frac{k'}{k_0}\cdot S_{\rm coh}(\mathbf{Q},\omega)\,, \tag{1b}$$

where $\sigma_{\rm inc}$ and $\sigma_{\rm coh}$ denote the incoherent and coherent cross sections and b is the scattering length of the nuclei. $|\mathbf{k}_0-\mathbf{k}'|\equiv|\mathbf{Q}|$ gives the wave vector transfer as neutrons of wave vector $\mathbf{k}_0$ (magnitude $2\pi/\lambda_0$) are scattered with a final wave vector $\mathbf{k}'(2\pi/\lambda')$. $S_{\rm inc}(\mathbf{Q},\omega)$ and $S_{\rm coh}(\mathbf{Q},\omega)$ are the scattering functions for the incoherent and coherent scattering and, in the case of a liquid, are dependent only on the magnitude Q of the wave vector transfer and the energy transfer taking place in the scattering process.

Van Hove has shown that the functions $S_{\rm inc}(\mathbf{Q},\omega)$ and $S_{\rm coh}(\mathbf{Q},\omega)$ are connected to the time-dependent correlation functions, $G_s(\mathbf{r},t)$—the self-correlation—and $G(\mathbf{r},t)$—the pair correlation—through Fourier transforms as follows:

$$G_s(\mathbf{r},t)=\frac{1}{(2\pi)^4}\int S_{\rm inc}(\mathbf{Q},\omega)\times\exp[-i(\mathbf{Q}\cdot\mathbf{r}-\omega t)]d\mathbf{Q}d\omega\,, \tag{2a}$$

and

$$G(\mathbf{r},t)=\frac{1}{(2\pi)^4}\int S_{\rm coh}(\mathbf{Q},\omega)\times\exp[-i(\mathbf{Q}\cdot\mathbf{r}-\omega t)]d\mathbf{Q}d\omega\,. \tag{2b}$$

Van Hove has further shown that the functions $G_s(\mathbf{r},t)$ and $G(\mathbf{r},t)$ have simple physical meanings for *classical liquids*. $G_s(\mathbf{r},t)$ represents the probability of finding an atom, which was at the origin at zero time, at the position $\mathbf{r}$ at time t. On the other hand, $G(\mathbf{r},t)$ represents the probability of finding *any* atom at $\mathbf{r}$ at time t when it is known that there was *an* atom at the origin at zero time. Obviously $G(\mathbf{r},t)$ includes $G_s(\mathbf{r},t)$ and it is possible to write $G(\mathbf{r},t)=G_s(\mathbf{r},t)+G_d(\mathbf{r},t)$. It is clear then, that if there was an atom at the origin at zero time, then $G_d(\mathbf{r},t)$ represents the probability of finding a *different* atom at the position $\mathbf{r}$ at a later time t.

At zero time $G_s(\mathbf{r},t)$ is a δ function and $G_d(\mathbf{r},t)$ reduces to the radial distribution function, as determined often from coherent x-ray scattering measurements. For a classical liquid Eqs. (2a) and (2b) can be separated into two parts and written in the form

$$G(r,t)=\frac{1}{2\pi^2}\int_0^\infty I(Q,t)\frac{\sin Qr}{Qr}Q^2dQ \tag{3}$$

and

$$I(Q,t)=\int_{-\infty}^{\infty}S(Q,\omega)\cos\omega t d\omega\,, \tag{4}$$

with the proper subscripts attached to $S(Q,\omega)$, $I(Q,t)$ and $G(r,t)$. In writing Eq. (3) use has been made of the fact that $I(Q,t)$ is independent of the direction of $\mathbf{Q}$.

If the specimen scattered purely incoherently, then Eqs. (3) and (4) would give $G_s(r,t)$. For a purely coherent scatterer, on the other hand, one would get $G_s(r,t)+G_d(r,t)$. In the general case, when incoherent as well as coherent scattering is present, use of Eq. (4) with

$$\left[\frac{1}{\langle b^2\rangle}\{(\langle b^2\rangle-\langle b\rangle^2)S_{\rm inc}(Q,\omega)+\langle b\rangle^2S_{\rm coh}(Q,\omega)\}\right]$$

will give the weighted combination

$$[G_s(r,t)+(\langle b\rangle^2/\langle b^2\rangle)G_d(r,t)].$$

It is possible then to separate $G_s(r,t)$ and $G_d(r,t)$ provided the two do not overlap. As we shall see this is true for much of the time range of interest to us.

Theoretically, the shape and width of the self-correlation function has been discussed by several authors based on special models for the liquid. It was shown by Van Hove[1] that at very small times ($\sim10^{-13}$ sec) the correct $G_s(\mathbf{r},t)$ should be given on the basis of a perfect gas model regardless of the state of the system. In this model,

$$G_s(\mathbf{r},t)=\left(\frac{M}{2k_BT\pi t^2}\right)^{3/2}\exp\left(-r^2\Big/\frac{2k_BT}{M}t^2\right). \tag{5}$$

On the other hand, at very large times, one expects that the classical equation of diffusion holds and in that case[2,8]

$$G_s(\mathbf{r},t)=\left(\frac{1}{4\pi D|t|}\right)^{3/2}\exp\left(\frac{-r^2}{4D|t|}\right), \tag{6}$$

where D is the diffusion constant of the liquid. The width of G_s, defined as the radius at which G_s has dropped by e^{-1}, is then given by

$$W_{1/e}=2(D|t|)^{1/2}. \tag{7}$$

[8] G. H. Vineyard, Phys. Rev. **110**, 999 (1958).

It can also be easily shown that in this model the full width of $S_{inc}(Q,\omega)$ at half-maximum is given by

$$\Delta E = 2\hbar DQ^2. \quad (8)$$

We shall not give the results which have been derived on the basis of more complicated models since it does not seem necessary to consider these models for the case of liquid argon.

III. APPARATUS AND EXPERIMENTAL DETAILS

A. Sample

In Fig. 1 we show the general flow diagram of the argon liquification system used for the experiment. Argon for all the experiments was liquified *in situ* in a liquid nitrogen cryostat also shown in Fig. 1. The pressure at the top of the boiling liquid argon was controlled by means of a pneumatic controlled valve and a Foxboro pressure controller. In most of the measurements the vapor pressure of argon was controlled at 550±10 mm of Hg giving a temperature of 84.5°K. In principle, it should not be necessary to use the helium reservoir shown in the figure. It was, however, noticed that whenever liquid nitrogen was added to the cryostat there was a tendency for the argon vapor in the chamber to freeze and thus to lower the pressure to a large extent (typically by 20 mm) which would then take a long time to build up again. On adding liquid nitrogen to the cryostat three to four times over a period of about 12 h this could make the vapor pressure go below the vapor pressure at the triple point (~520 mm) and the argon would freeze. By connecting the helium reservoir we were able to bring the pressure drop down to 10 mm and the pressure build up also was quicker. With this system it was easily possible to control the vapor pressure at 550 mm to within ±10 mm of mercury. By means of a glass window on top of the liquid argon chamber we could also visually make sure that there was no freezing at any time and that the liquid was in a boiling condition.

The specimen holder itself was a cylindrical aluminum container, 2.5 cm in diameter and 7.5 cm in height. Since we were very concerned about the multiple scattering from the specimen, a special design was adopted for the container.[9] The whole container was separated into eight compartments by means of thin cadmium absorbers placed horizontally $\frac{3}{8}$-in. apart. We estimate multiple scattering to be only about 3–4% of the primary scattering. We may remark here that while trying to eliminate multiple scattering we have also reduced the primary scattering to a large extent. As a result we were not able to collect data with statistics as good as we had hoped. Nevertheless, we think that the final results are accurate to about 10% in the transformed quantities.

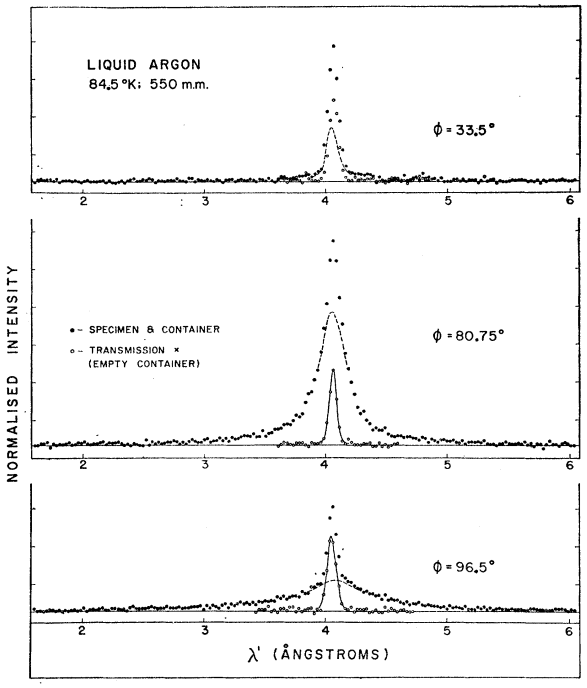

FIG. 2. Wavelength distributions observed with the rotating-crystal spectrometer.

Extending below the specimen container was a similar dummy container which also had cadmium partitions similar to the sample container. By lowering and raising the cryostat automatically we could take readings at intervals for the specimen and its container, and for an empty container in the beam.

The gas used was supplied by Matheson Gas Company. A fresh specimen of liquid argon was prepared at intervals of about five days.

B. Rotating Crystal Spectrometer

The details of the rotating crystal spectrometer installed at the NRU reactor at Chalk River have been described earlier[10] and we will just give the main features here. The rotating crystal gives bursts of neutrons of 4.05_9 Å selected out of a beryllium-filtered spectrum. These neutrons, after being scattered from the specimen, travel a distance of about 3.3 m before they are detected in a bank of $B^{10}F_3$ counters. There are three sets of counters each covering an angular range of 2.25° in the horizontal direction. The resolution of the spectrometer is ~2% in wavelength or $\sim 2\times 10^{-4}$ eV at the incident energy.

Wavelength distributions of 4.05_9 Å neutrons scattered from the liquid argon under its own saturated

[9] B. N. Brockhouse, J. Bergsma, B. A. Dasannacharya, and N. K. Pope, *Inelastic Scattering of Neutrons in Solids and Liquids* (International Atomic Energy Agency, Vienna, 1963), Vol. 1, p. 189.

[10] B. N. Brockhouse, in *Inelastic Scattering of Neutrons in Solids and Liquids* (International Atomic Energy Agency, Vienna, 1961), p. 113.

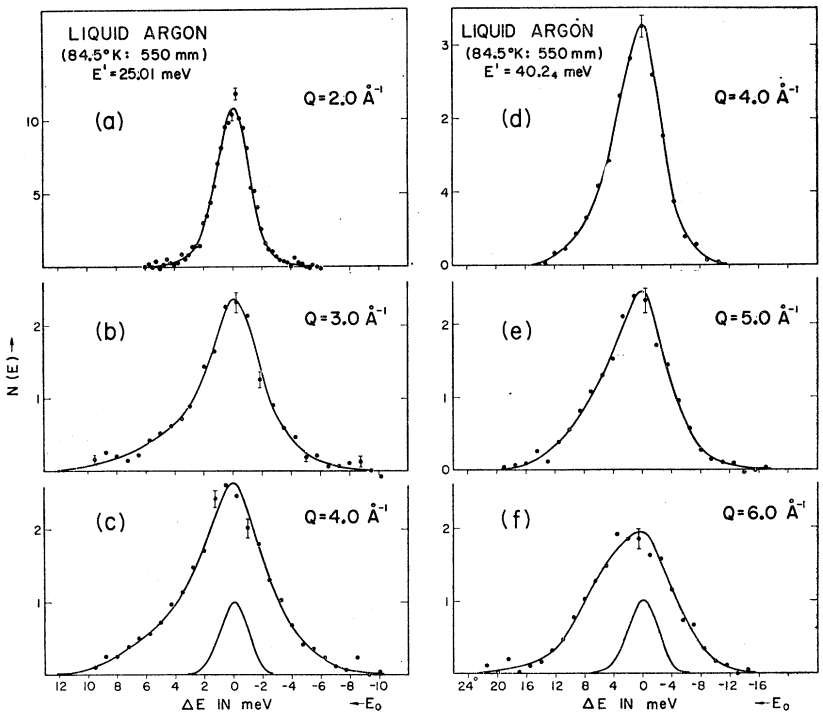

FIG. 3. Typical constant-Q energy distributions observed with the triple axis spectrometer. (c) and (f) also show the resolution function for the two outgoing energies.

vapor pressure (550 mm, equivalent to 84.5°K) have been measured at about twenty angles of scattering between 17° and 110°. Typical normalized distributions are shown in Fig. 2 (filled circles) together with similar patterns taken for empty containers (open circles). These patterns have already been corrected for the k'/k_0 factor and for the calculated efficiency variation of the counter, etc. The fast-neutron background was measured for each run by inserting a cadmium shutter in the monochromatic beam for half a minute at intervals of five minutes. The flat background is also indicated in Fig. 2 and was removed before subtracting the normalized empty container counts (corrected for transmission of the specimen[11]) from the counts obtained with both the specimen and the container in the beam. This difference is shown by dashed lines. The angular range covered by the detectors at any scattering angle in most of these measurements was 6.75° comprising three sets of detectors each covering 2.25°. Near the first peak in the diffraction pattern of liquid argon (scattering angle, $\phi=80.75°$, $Q=2.0$ Å^{-1}) these three sets could be separated because of better available intensity. Five of the wavelength distributions were measured in this way.

We may remark here that we had some difficulty in the subtraction of the empty-container counts in the elastic channels. In order to check this we took the actual container counts (instead of the dummy) at liquid-nitrogen temperature to carry out the subtraction. This did not introduce any appreciable improvement. However, we were able to draw smooth curves through these channels since the number of channels affected by this is few (~3 or 4 channels). We do not think that this has introduced any appreciable error in the transformed quantities. This experiment covers a wave vector transfer range from 0.4 to 2.2 Å^{-1}.

The resolution of the spectrometer as a function of scattering angle was measured using a specimen which consisted of polythene sheet rolled into a number of concentric cylinders, the outermost having 2.5 cm outer diameter and 7.5 cm high, the same dimensions as the argon scatterer. It was found that the distributions of the elastic component measured with this specimen were Gaussian within experimental error.

C. Triple-Axis Spectrometer

The details of the triple axis spectrometer at the NRU reactor have also been described earlier.[10] It was our intention to measure the energy distributions of neutrons for wave vector transfers Q up to 6.0 Å^{-1}, a range of Q covering the first three maxima in the liquid-argon diffraction pattern. The range of measurements covered on this spectrometer was from 1.8 to 6.0 Å^{-1} making use of two fixed outgoing wavelengths for different ranges of Q.

All the measurements were made using the "Constant Q" mode of operation of the spectrometer[10,12] with the

[11] B. N. Brockhouse, L. M. Corliss, and J. M. Hastings, Phys. Rev. 98, 1721 (1955).

[12] B. N. Brockhouse, T. Arase, G. Caglioti, K. R. Rao, and A. D. B. Woods, Phys. Rev. 128, 1099 (1962).

outgoing wavelength kept constant during any one run, and using constant energy steps in the incoming monochromatic beam. The method of variable energy incoming beam has the advantage[10] that, insofar as a monitor counter with a $1/v$ efficiency is used in the monochromatic incident beam, it is possible to eliminate experimentally the k'/k_0 factor which appears in the cross section formula [Eq. (1)]. A U^{235} fission counter was used for this purpose. Thus, with this spectrometer it is possible to observe directly $S(Q,\omega)$, folded, of course, with the resolution.

An outgoing neutron wavelength of 1.80_8 Å ($E'=25.0$ meV) was used to study energy distributions from $Q=1.8$ to 4.0 Å^{-1} at intervals of Q equal to 0.2 Å^{-1}. Some typical distributions are shown in Fig. 3. In all the distributions with $\lambda'=1.80_8$ Å the readings were taken at steps of energy equal to 0.25 meV as shown for the case of $Q=2.0$ Å^{-1} (note that the intensity here is higher than in other cases; this Q corresponds to the first peak of the diffraction pattern). At every point the counts were first recorded with the specimen and the container both scattering neutrons and then with the dummy container alone in the neutron beam. The counts with the dummy container were subtracted point by point from the counts with the specimen plus container after applying a transmission correction[11] (transmission $\sim 94\%$) to the latter. Where the energy distributions have considerably greater energy width than that for $Q=2.0$ Å^{-1}, three consecutive points have been averaged before plotting.

Also shown in the figure is the resolution function taken with a vanadium powder specimen. The vanadium powder was contained between two thin aluminum cylinders made with foils of 0.002-in. thickness and with a $\frac{1}{8}$-in. gap in between them. The diameter of the outer cylinder was 2.5 cm, i.e., the same as that of the argon specimen. The resolution was measured at several values of Q (taking care that Q was not close to any of the Bragg reflections of aluminium); it was found that the resolution function is independent of Q. The resolution function shown has a full width of 2.35 meV at half-maximum which corresponds to a wavelength resolution of approximately 4.6%. In the figure, negative ΔE denotes an energy gain process.

It is known that crystal spectrometers suffer from order contamination problems. In order to overcome this trouble we used, in the main reactor beam, a filter composed of $9\frac{1}{2}$ in. of quartz single crystals. Measurements made earlier at the NRU reactor indicate that with such a filter, about 3.5% of the monitor counts at 25 meV come from neutrons reflected in the second order of monochromator crystal. This contamination will introduce errors in our experiments in two ways. Firstly, the normalization to fixed monitor counts will not be quite correct, since the fraction of second-order neutrons present in the incident beam changes as the incoming wavelength is varied while measuring any energy distribution. Secondly, the second-order neutrons themselves will have a scattered spectrum which could be detected (by second-order reflection of the analyzer) when the primary spectrum is being recorded in the vicinity of the elastic position. These two effects act in opposite directions. Energy and reflectivity considerations show that the second type of effect will be small compared to the first. No correction has been applied to the measured scattering function for this effect. Probably, this is the largest source of systematic error in the distributions.

Similar constant-Q energy distributions were taken at $Q=3.0$ Å^{-1} and in the range of Q from 4.0 to 6.0 Å^{-1} using $\lambda'=1.42_5$ Å ($E'=40.2$ meV) and are shown in the right half of Fig. 3. The energy distributions were again measured at intervals of Q equal to 0.2 Å^{-1}. In these distributions successive points were at energy intervals of 0.5 meV. In the figure three successive points have been averaged before plotting. The length of quartz single crystal in the beam in this case was reduced to 6 in., since the number of second-order neutrons at this energy is expected to be very small. Energy distributions at $Q=4.4$ and 5.2 Å^{-1} could not be taken since at these positions the aluminium container gives an intense Bragg reflection and subtraction of empty container counts becomes difficult. This is not a serious difficulty as will be seen in the next section.

The resolution measured using the same vanadium scatterer as earlier is also shown in the figure. The resolution is 4.95 meV in energy or about 6% in wavelength.

In order to be able to check the consistency of measurements we covered overlapping regions in Q whenever the instrument or the wavelength was changed. For example, energy distributions at $Q=1.8$, 2.0, and 2.2 Å^{-1} were measured using the rotating crystal spectrometer and the triple axis spectrometer with $\lambda'=1.80_8$ Å. Energy distributions at $Q=3.0$ and 4.0 Å^{-1} were measured using the triple axis spectrometer with $\lambda'=1.80_8$ Å and with $\lambda'=1.42_5$ Å. However, these distributions cannot be compared among themselves without making further assumptions, since they are folded with different resolutions. It can be seen easily, for any given resolution of a Gaussian shape, that the width will be larger if a Gaussian shape is assumed for the true distribution than if it is assumed to be a Lorentzian. The difference increases as the resolution becomes poorer. For this reason one would not be justified in comparing the width of these distributions straightaway under any of the above assumptions. The comparison has been done, however, after finding the intermediate scattering function (resolution removed) as discussed in the next section; good agreement was found.

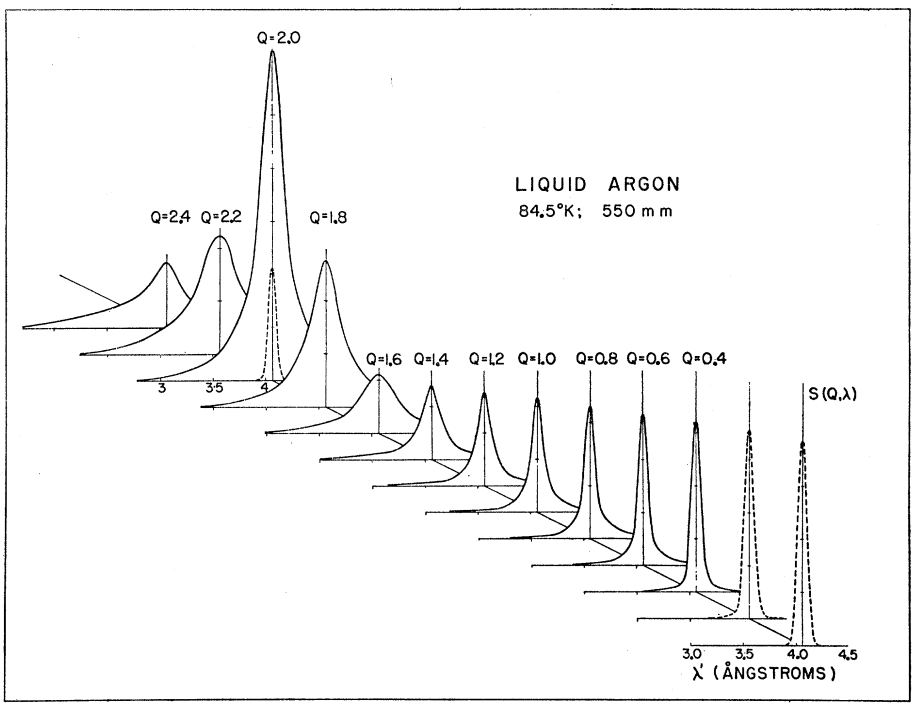

FIG. 4. The scattering surface for liquid argon plotted as a function of wave vector transfer Q and the wavelength λ' of the outgoing neutrons.

IV. ANALYSIS OF DATA AND RESULTS

A. Scattering Function

As pointed out earlier our main aim is to obtain the correlation functions, for which we need $S(Q,\omega)$ as a function of wave vector transfer Q and energy transfer $\hbar\omega$ for a wide range of Q.

The data obtained on the triple axis spectrometer gives us $S(Q,\omega)$ directly[10] as already explained. However, the data obtained on the rotating crystal spectrometer, after correction for efficiency variation of the detector, for the k'/k_0 factor, etc., gives the scattering function as a function of scattering angle and time-of-flight. This is easily converted to a true energy distribution. To further convert this to a function at a fixed wave vector transfer a procedure similar to that of Sakamoto *et al.*[13] was followed. A grid of Q versus $\hbar\omega$ was formed. The grid points were taken at intervals of 0.1 Å^{-1} in Q and 0.5×10^{-4} eV in energy. The scattering surface obtained this way is shown in Fig. 4. For convenience in drawing, $S(Q,\lambda')$ versus λ' has been plotted.

The dashed curves at $Q=0$ and 2.0 Å^{-1} show the resolution function for the spectrometer at the corresponding Q values, observed as described in Sec. III. The curve shown at $Q=2.0$ Å^{-1} is experimentally observed whereas the curve shown at $Q=0.0$ Å^{-1} is found by extrapolation. To get this resolution, the following procedure was followed. The full width at half-maximum of resolutions at different scattering angles was plotted as a function of $Q_0=4\pi\sin\frac{1}{2}\phi/\lambda_0$ (since the resolution width is only $\sim2\times10^{-4}$ eV, the Q variation can be neglected). The smooth curve was extrapolated to obtain the width of the resolution at zero wave vector transfer. It was further found that the resolution functions were Gaussian at all the measured values of Q_0. A Gaussian shape was therefore also assumed for the resolution at zero wave vector transfer. Now, it is known that the actual energy distribution at $Q=0$ is a δ function in energy, and so the observed distribution should be just the resolution itself. The area of this curve is then obtained by extrapolation of the observed diffraction pattern at low Q values [see Fig. 5(b)].

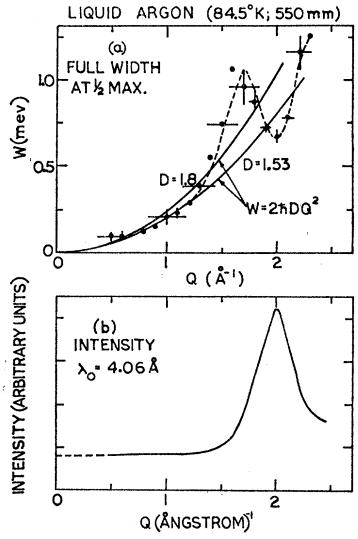

FIG. 5. (a) The full width at half-maximum of the distributions observed on the rotating crystal spectrometer. The full line shows the width expected on the basis of simple diffusion. The diffusion constant is expressed in units of 10^{-5} cm^2/sec. (b) The diffraction pattern of liquid argon.

[13] M. Sakamoto, B. N. Brockhouse, R. G. Johnson, and N. K. Pope, J. Phys. Soc. Japan **17**, Suppl. B II, 24 (1962).

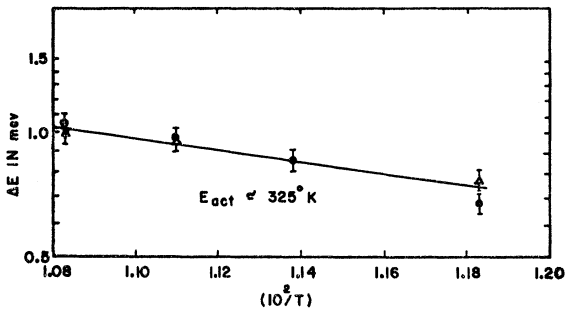

FIG. 6. Temperature dependence of the width of the wavelength distributions at scattering angles of 74 deg (triangles) and 83 deg (filled circles).

Thus, the dashed curve at zero wave vector transfer represents both the resolution and the energy distribution which should be observed at $Q=0.0$ Å^{-1}. The curve at $Q=0.2$ Å^{-1} was found by interpolation between $Q=0.0$ Å^{-1} and larger values of Q than 0.2 Å^{-1}. The distributions $S(Q,\omega)$ thus obtained can now be used for Fourier transformations to $I(Q,t)$ and $G(r,t)$ along with the data obtained on the triple axis spectrometer.

Before presenting the results of the Fourier transformation we shall examine the distributions themselves more closely. In Fig. 5(a) we have plotted the observed full widths at half-maximum of the distributions as a function of Q. The widths were obtained by assuming that the observed distributions are a convolution of a Lorentzian with a Gaussian resolution. The bars indicate the estimated error in widths and the resolution in Q.

Figure 5(b) shows the observed diffraction pattern using the same instrument. At small Q the scattering is almost completely incoherent. In this region we note from Fig. 5(a) that the widths probably have the value $2\hbar DQ^2$ expected on the classical diffusion model of the liquid. The values of D used in drawing the curves are shown[14,15] in the figure. There exists another measurement of D, at a single temperature, giving a value of 2.07×10^{-5} cm^2/sec.[16]

As one approaches higher values of momentum transfer the coherent effects are clearly visible as an oscillation in the width of the energy distributions. Exactly at $Q=2.0$ Å^{-1}, where the diffraction pattern is a maximum, the width shows a minimum as predicted by DeGennes.[7] This type of narrowing has been seen in lead[3] earlier. A rough comparison of the energy widths with those given by DeGennes shows that the experimental values in the range of Q from 1.75 to 2.25 Å^{-1} are smaller by approximately 10%.

Another point worth noting about the distribution is the absence of any obvious inelastic structure in the distributions unlike those found in sodium[6] and tin[5] near the melting point in a similar experiment. The inelastic scattering, if it is present, should probably show up in the region less than the energy transfer (~7 meV) which corresponds to the Debye temperature of solid argon. The lack of inelastic scattering probably points towards "looseness" of the liquid structure and the simple behavior of atomic motions in liquid argon.

Some time-of-flight distributions were also measured at temperatures corresponding to saturated vapor pressures of 800, 1000, and 1250 mm of Hg, for angles of scattering equal to 74° and 83°. These scattering angles are close to the position of the first peak in the diffraction pattern. The full width at half-maximum of these distributions are plotted on a logarithmic scale as a function of $1/T$ in Fig. 6. Within the experimental errors a straight line is fitted from the slope of which an activation energy of about 700 ± 200 cal/mole can be derived. This, within our large experimental errors, is in agreement with values derived from measurements on temperature dependence of the self-diffusion coefficient of liquid argon.[14,15] This is in spite of the fact that at these angles a large degree of DeGennes[7] narrowing occurs because of coherence in the scattering. This result is in contrast with those obtained from measurements on lead[4] and tin,[4] for which activation energies derived from neutron measurements were found to be smaller by about a factor of two than those deduced from measurements of self-diffusion.

B. Intermediate Scattering Function

Coming back to the Fourier transformation[17] of the data, the function $I(Q,t)$ calculated using Eq. (4) is shown in Fig. 7, for different times, after removing the resolution. The resolution was removed by dividing the

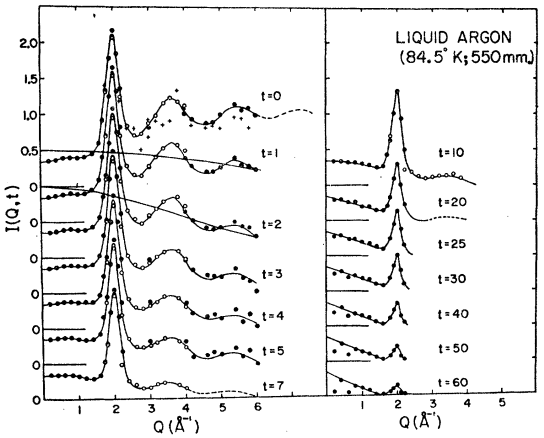

FIG. 7. The intermediate scattering function for different times (in units of 10^{-13} sec). Circles are the direct results of our experiments. Crosses at zero time are deduced from second moments of the observed distributions. The Gaussians at $t=1\times10^{-13}$ sec and $t=2\times10^{-13}$ sec are calculated using a perfect gas model for the liquid.

[14] G. Cini-Castagnoli and F. P. Ricci, Nuovo Cimento **15**, 795 (1960).
[15] J. Naghizadeh and S. A. Rice, J. Chem. Phys. **36**, 2710 (1962).
[16] J. W. Corbett and J. H. Wang, J. Chem. Phys. **25**, 422 (1956).
[17] These transforms were all done on the Datatron computer at Atomic Energy of Canada, Chalk River Limited.

cosine transform [Eq. (4)] of the scattering function observed with the specimen in the beam by the cosine transform of the resolution function.

All the points at $t=0$ were normalized with respect to the diffraction pattern observed by us and, earlier, by Henshaw.[18] The statistics on the diffraction pattern observed by us were somewhat better than on that reported by Henshaw. For normalization, the ratio of $I(Q,0)$ to the observed diffraction pattern was calculated for every observed point on the $I(Q,0)$ curve. The average of this ratio was used for normalization. The deviation of points from the observed diffraction pattern was less than 5% on an average for each one of the three sets (one set of data taken on the rotating crystal spectrometer and two sets on the triple-axis spectrometer). The dashed part of the $I(Q,0)$ curve was obtained by using x-ray data of Eisenstein and Gingrich[19] on liquid argon and neutron data of Clayton and Heaton[20] on liquid krypton.

The filled circles in the Q range from zero to 2.2 Å^{-1} are those obtained from rotating crystal spectrometer data, the open circles were calculated by utilizing the data obtained on the triple-axis spectrometer at the fixed out-going neutron wavelength λ' of 1.80_8 Å and the remaining filled circles were got by using λ' equal to 1.42_5 Å, again on the triple-axis spectrometer. We notice that the data obtained using quite different resolutions are consistent within experimental errors.

The normalization factor calculated for $I(Q,0)$ has also been used for normalizing the intermediate scattering function at finite times (Fig. 7). As remarked in the previous section we have made measurements over overlapping regions of $Q(=1.8, 2.0, 2.2, 3.0, 4.0$ Å$^{-1})$ so that data taken independently could be compared. We find a good over-all agreement between the values of $I(Q,t)$ at all times for these values of wave vector transfer. The consistency between these results of independent measurements gives confidence in the procedure of Fourier transformation.

The reason for the comparatively faster fall of $I(Q,t)$ at $Q=3.6$ Å^{-1}, with increasing time is not understood and these points have been ignored in drawing the smooth curves through the points.

A further check on the data is provided by use of the moment theorem of DeGennes,[7]

$$I(Q,0)=\frac{k_BT}{M}\frac{(\hbar Q)^2}{\langle(\hbar\omega)^2\rangle}. \tag{9}$$

The crosses in Fig. 7 show the points calculated in this way (the resolution has been removed by assuming distribution folded to a Gaussian resolution). The agreement is considered to be fair. A more detailed examination of the data shows that the consistently lower values of the crosses on the figure is largely due to the assumption that the distribution which is being unfolded is a Gaussian.

It has been shown by Van Hove that for classical systems at small times the self-correlation function is independent of the state of the system, so that for small t and large Q

$$I(Q,t)=\exp\left[-\frac{k_BT}{M}Q^2t^2\right]. \tag{10}$$

The observed $I(Q,1)$ and $I(Q,2)$ and the curves calculated from Eq. (10) are also shown in Fig. 7. It is seen that the observed curves asymptotically tend to the value given by the above equation.

At times larger than 10×10^{-13} sec the results from the triple axis spectrometer (for which the resolution is much less good) cannot be used in the transforms; therefore for $t\geqslant 20\times10^{-13}$ sec an arbitrary extrapolation has been made from Q equal to 2.2 to 4.0 Å^{-1}. It is assumed that at still larger times this part is zero.

C. Correlation Functions

It is a straightforward procedure[21] now to calculate by means of Eq. (3), the correlation functions from the observed intermediate scattering functions, $I(Q,t)$. For the practical reason that it is not possible to observe the intermediate scattering function for all values of Q, a modified form of Eq. (3) was used, in which the upper limit of the integral was replaced by $Q_{\max}$, the largest experimentally observed value of Q (instead of infinity). The errors that are introduced by such a termination of the data have been discussed in great detail in the literature and will not be treated here. It will be enough to remark that this error will affect the results only at times less than 5×10^{-13} sec since at larger times $I(Q,t)$ tends to zero within the Q range of our observation. The effect of termination can be seen as spurious oscillations in the $G(r,t)$ curves.

As remarked in Sec. II, one arrives at a weighted combination of the self- and pair-correlation functions when the total scattering function (coherent plus incoherent) is used in Eq. (4). It is clear, however, that if one knows the ratio of $\langle b\rangle^2$ to $\langle b^2\rangle$ it is possible to determine completely $G_s(r,t)$ and $G_d(r,t)$ over times for which the two functions do not overlap. The ratio $\langle b\rangle^2/\langle b^2\rangle$ can be easily found from the diffraction pattern of liquid argon; large angle scattering from the liquid is proportional to $\langle b^2\rangle$ and the zero angle scattering, which is almost completely incoherent, is proportional to $\langle b^2\rangle-\langle b\rangle^2$. The knowledge of these two immediately gives the required ratio. A value 0.66 derived from the observed diffraction pattern was used for this ratio in all the calculations. In this way a complete separation of G_s and G_d has been made for time from zero to 10^{-12} sec; G_d in this time range is shown

[18] D. G. Henshaw, Phys. Rev. **105**, 976 (1957).
[19] A. Eisenstein and N. S. Gingrich, Phys. Rev. **62**, 621 (1942).
[20] G. T. Clayton and L. Heaton, Phys. Rev. **121**, 649 (1961); also see Argonne National Laboratory Report No. 6112 (unpublished).
[21] Transformation from $I(Q,t)$ to $G(r,t)$ was done on the TIFRAC computer at the Tata Institute of Fundamental Research, Bombay, India.

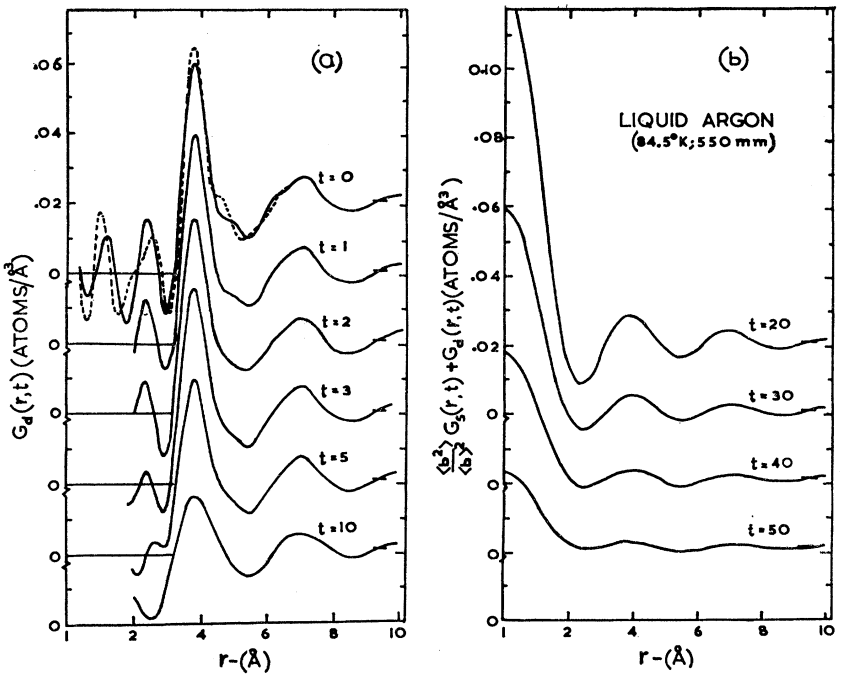

FIG. 8. (a) Pair distribution function for different times (in units of 10^{-13} sec). (b) A weighted combination of the self- and pair-correlation functions for large times.

in Fig. 8(a), G_s in the same range has been plotted in Fig. 9. Figure 8(b) shows the combination $[(\langle b^2\rangle/\langle b\rangle^2)G_s+G_d]$ in the time range of 20×10^{-13} to 50×10^{-13} sec. It is still probably possible to separate G_s and G_d at $t=20\times10^{-13}$ sec.

$G_d(r,0)$: The pair-correlation function at zero time is calculated in the standard fashion by using[22] $[I(Q,0)-I(\infty,0)](\langle b^2\rangle/\langle b\rangle^2)$ in place of $I(Q,t)$ in Eq. (3) and replacing the upper limit of the integral by the maximum observed value of Q. The curve thus obtained is shown in Fig. 8(a). The full curve (at $t=0$) is the result got by taking the complete data from our measurements, which give $I(Q,0)$ up to a maximum value of $Q=6.0$ Å^{-1}. The dashed curve is obtained using the extrapolated $I(Q,0)$ shown in Fig. 7. The difference between these two patterns is consistent with what one expects from such a termination of data. The first peak is at 3.80 and 3.76 Å, respectively, for the two curves. On the other hand the distance of closest approach on the basis of the two curves is 3.16 and 3.24 Å, respectively. These results are generally in agreement with the results of Eisenstein and Gingrich[19] and Gingrich and Tompson[23] on liquid argon. Gingrich finds the first peak at 3.78 Å; Henshaw gives the above two distances as 3.86 and 3.05 Å, respectively. (Gingrich and Tompson give a discussion of their results and those of Henshaw.) We also notice the oscillations in the $G_d(r,0)$ for values of $r\lesssim3$ Å, which arise because of termination of $I(Q,0)$ and are spurious. The amplitude of these oscillations is larger than those reported in earlier experiments. The reason for this is not known. Several slightly different values of $I(\infty,0)$ were used in order to see the effect of taking a wrong asymptotic value of the intermediate scattering function on these oscillations and in general on the pair-correlation function. This did not appreciably reduce the oscillations. The curve shown in the figure was obtained by using a value of $I(\infty,0)$ such that the criterion

$$-2\pi^2\rho=\frac{\langle b^2\rangle}{\langle b\rangle^2}\int_0^{Q_{\max}}Q^2[I(Q,0)-I(\infty,0]dQ$$

is nearly satisfied. ρ denotes the density of the liquid.

It is also possible to compare the pair-correlation function at zero time obtained for different inert elements by making use of the principle of corresponding states. This has been done, using Henshaw's data for argon, neon, and helium by Ricci,[24] who finds good agreement between the distributions of the two heavier elements. We have compared our data similarly with those of Clayton and Heaton[20] on krypton and the comparison is shown in Fig. 10. We find good agree-

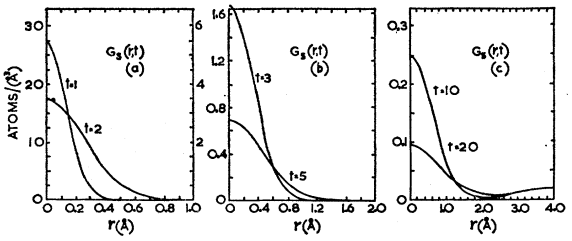

FIG. 9. Self-correlation function for different times (in units of 10^{-13} sec). The ordinate on the right-hand axis of (a) applies to $t=2\times10^{-13}$ sec.

[22] $I(\infty,0)$ has been normalized to one.

[23] N. S. Gingrich and C. W. Tompson, J. Chem. Phys. **36**, 2398 (1962).

[24] F. P. Ricci, Nuovo Cimento **16**, 532 (1960).

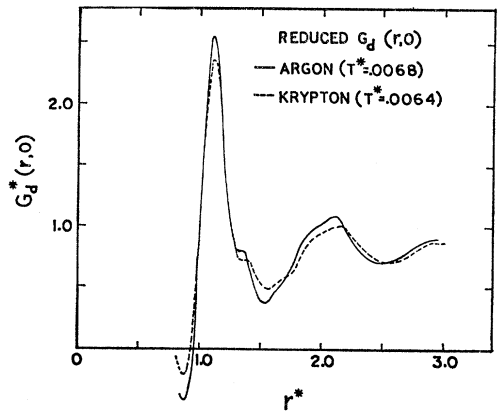

FIG. 10. The reduced pair distribution function for liquid argon (———) and liquid krypton (– – – – –). Liquid-argon distribution is derived from our measurements and the liquid-krypton distribution from those of Clayton and Heaton (Ref. 20).

ment between the results. Similar comparison can be made at finite times, as shown by Vineyard.[25]

$G_d(r,t)$: Just as one used $I(Q,0)-I(\infty,0)$ in the integral for getting the $G_d(r,0)$, it is useful[3] to take differences of the type $[I(Q,t)-I_g(Q,t)]$ at small times. For times 1×10^{-13} and 2×10^{-13} sec the Gaussian distributions to which $I(Q,t)$ tends asymptotically at large Q, have been chosen as $I_g(Q,t)$. At $t=3\times10^{-13}$ sec a similar Gaussian with a different effective t was chosen. From times 5×10^{-13} sec onwards one need not take such differences since the data themselves are complete and termination errors have almost vanished.

The pair-correlation functions at finite times show the same general behavior as $G(r,0)$. The position of the first peak remains the same. As time increases the peak heights fall and the valleys fill up. The width of the peak increases with time. All this is consistent with the qualitatively expected behavior of $G_d(r,t)$.

$G_s(r,t)$: As remarked in the beginning of this section, it is possible to separate completely G_s and G_d for times from 0 to 20×10^{-13} sec. The self-correlation functions thus found are plotted in Fig. 9.

By fitting we find that these are all Gaussian in shape to within our experimental accuracy.

The function G_s should satisfy the condition

$$\int 4\pi r^2 G_s(r,t)dr=1. \qquad (11)$$

It is easy to find the value of the integral knowing the width and the peak height of G_s since the self-correlation is found to be Gaussian. We find the value of the experimentally found integral to be unity to within 10% for all values of $t\leqslant 20\times10^{-13}$ sec. This is true though no special normalization has been done except that described in Sec. IV B; this fact gives confidence in the essential reliability of the results. It further tends to show that even at the fairly large time of 20×10^{-13} sec, the overlap of G_d and G_s is not large enough to prevent getting the correct half-width of the self-correlation function. These widths of the self-correlation function are plotted in Fig. 11.

The observed widths at 25×10^{-13} sec onwards are probably affected by the overlapping $G_d(r,t)$ as indicated by the experimentally found value of the above integral. Now, if the reasonable assumption is made that at these fairly large times G_s is Gaussian, then one can find the width by a knowledge of just the peak height and the use of Eq. (11). The radii of the self-correlation function found in this way are marked with open circles. It is not possible to get the width at 50×10^{-13} sec since it is felt that even the peak height of G_s is affected by the overlap of G_d.

It is interesting to compare the curve of Fig. 11 with calculations for theoretical models. The straight line in Fig. 11 shows the theoretically calculated width for argon gas. At small times there is good agreement with the gas model. If one assumes a simple classical model for the liquid, the diffusion being given by Fick's law, the behavior of the half-width of G_s can be easily calculated using the measured value of the self-diffusion constant [Eq. (7)]. The three parabolas show the calculated values corresponding to three different values of measured diffusion constant. The curve given by $D=1.8\times10^{-5}$ cm^2/sec most nearly follows the experimental points. (However, see the remarks about Fig. 5.) This curve shows that in argon diffusion takes place in a very simple way. This might be expected in a liquid like argon which consists of spherically symmetric, monoatomic molecules with weak forces between them. The activation energy measured from temperature dependence of diffusion constant and from our measurements (Fig. 6) shows a value of about 30 meV. Considering the fact that thermal vibrations in solid argon have energies of the order of 10 meV (the Debye temperature is ~80°K) fairly free diffusion may be expected. Such a suggestion was made earlier by Cini-Castagnoli and Ricci[14] on the basis of diffusion measurements.

V. SUMMARY AND CONCLUSIONS

The energy distributions of neutrons scattered from liquid argon were found to be of very simple nature in the sense that no obvious inelastic structure could be seen in the distribution. Such a component has been seen in sodium[6] and tin[5] in the liquid phase just above the melting point. This absence of structure itself points toward the simple diffusive properties of liquid argon. The width at half-maximum of the scattering function has been examined and it is found that the full width at half-height as a function of the momentum transfer follows approximately a simple parabolic law given by $\Delta E=2\hbar DQ^2$ for small values of momentum transfer. (In this region the scattering is mostly incoherent.) In the region of the first diffraction maximum the DeGennes type of narrowing is observed;

[25] G. Vineyard, Phys. Rev. **119**, 1150 (1960).

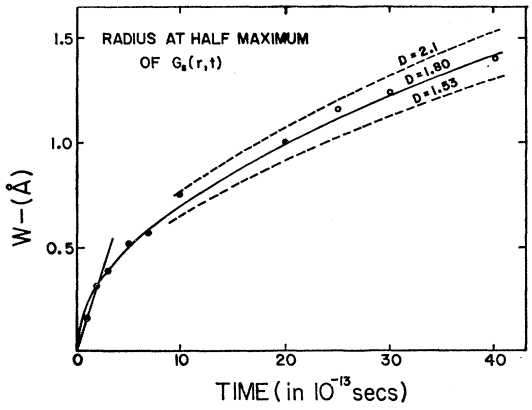

FIG. 11. The width at half-maximum of the self-correlation function as a function of time. The open circles are derived as described in text.

however, the energy width of the scattering function observed in this region is lower than that calculated by DeGennes by about 10%.

The scattering function, $S(Q,\omega)$ was converted to the intermediate scattering function, $I(Q,t)$ by a cosine transformation over energy transfer. Checks have been applied on the nature of $I(Q,t)$ mainly by examining $I(Q,0)$, $I(Q,1)$ and $I(Q,2)$. $I(Q,0)$ must be the same as the ordinarily observed diffraction pattern, and $I(Q,1)$ and $I(Q,2)$ must tend asymptotically to values given by the perfect gas model for the liquid. Also, different instruments were used which covered overlapping regions of momentum-transfer. At all times good agreement was found between the $I(Q,t)$ values calculated from these different measurements even though normalization for the intermediate scattering function was done only at zero time. The checks and the over-all consistency of data obtained independently suggest that our results are probably correct to about 10 to 15%.

The main result of the experiment is the complete mapping of the time-dependent correlation functions of Van Hove (Figs. 8 and 9). The pair-correlation function at zero time can also be found from x-ray measurements; our measurements are in agreement with earlier x-ray measurements and give the distance of the first neighbor to be 3.76 and 3.80 Å, respectively, for the two slightly different sets of data. The distance of closest approach, from the same patterns, is given to be about 3.2 Å. These results are also in agreement with those on krypton if one compares the results, making use of the principle of corresponding states (Fig. 10).

It has been possible to completely separate the self and pair parts of the correlation function in the time range of 0 to 20×10^{-13} sec, an important time range for the diffusive properties of the liquid. The self-correlation function is found to be Gaussian in this range of time. Now, if there is an atom at origin at zero time then the probability of finding the same atom somewhere in space at any later time is unity. The self-correlation function calculated from our measurements satisfies this normalization condition to about 10% automatically for all times up to 20×10^{-13} sec. The deviation from the normalization condition points to the extent of error in the correlation function. The width at half-maximum of the self-correlation function has been plotted and compared with widths theoretically predicted on the basis of the model of simple diffusion (Fick's law). The agreement is found to be good within experimental errors, even at rather small times (see Fig. 11) for $D=1.8$ cm^2/sec and it is concluded from this that in liquid-argon diffusion probably takes place in a simple way, without jumps[2] or diffusion of "globules."[26] It is very likely that this will be true of other heavy inert elements also, since they are known to follow the law of corresponding states for static as well as transport properties. The present result is unlike that found for liquids like water, liquid lead, and liquid sodium where the width function over similar time scale does not follow the simple diffusion formula. This deviation from simple diffusion theory arises because of the existence of cooperative effects, which seem to be small for liquid argon. Very recent calculations of Rahman,[27] however, suggest that such effects exist in liquid argon also. *Note added in proof.* A fit of the type $(W)^2=At+\epsilon$ at large times gives a value of diffusion coefficient $D=1.58\times10^{-5}$ cm^2/sec and $C=0.15$ Å and suggests a delay time of 1×10^{-12} sec for diffusion to set in. This makes Figs. 5 and 11 consistent.

A limited study was made of the variation of the scattering function with temperature. An activation energy of about 700 ± 200 cal/mole has been calculated from these measurements in agreement with measurements on the macroscopic diffusion constant. This agreement is consistent with a simple behavior of diffusion. This is interesting especially in view of similar measurements on lead[4] and tin[4] where serious disagreement was found between neutron and diffusion coefficient measurements and in which the diffusion process is consequently thought to be comparatively complicated.

ACKNOWLEDGMENTS

The authors are deeply indebted to Professor B. N. Brockhouse for his guidance, keen interest and help during the course of this work. We wish to thank Dr. N. K. Pope for many helpful discussions and for the Fourier transformation program for the Datatron, Dr. A. D. B. Woods for helpful discussions, Natesh Kumar for writing the Fourier transformation program for the TIFRAC and E. A. Glaser, A. L. Bell, and R. Rea for technical assistance. We are thankful to the Colombo Plan authorities for financial assistance and the Atomic Energy of Canada Limited for hospitality during our stay.

[26] P. A. Egelstaff, Advan. Phys. **11**, 203 (1962).
[27] A. Rahman, Phys. Rev. **136**, A405 (1964).